The Interaction of Porcine Dihydropyrimidine Dehydrogenase with the Chemotherapy Sensitizer:

5-Ethynyluracil

Dariush C. Forouzesh¹, Brett A. Beaupre¹, Arseniy Butrin¹, Zdzislaw Wawrzak²,

Dali Liu¹ and Graham R. Moran¹*

- 1. Department of Chemistry and Biochemistry, 1068 W Sheridan Rd, Loyola University Chicago, Chicago, IL 60660
- 2. Northwestern University, Synchrotron Research Center, Life Sciences Collaborative Access Team, Argonne, IL 60439, USA.

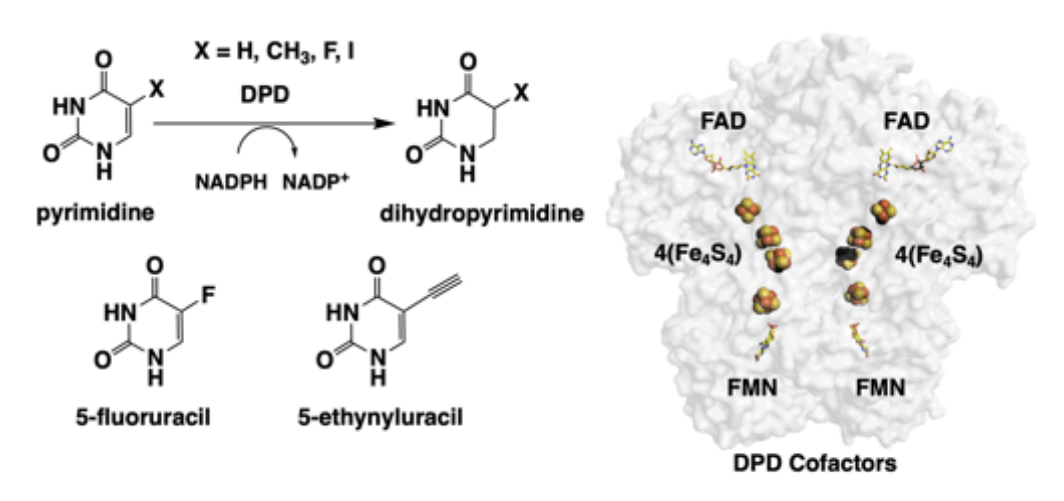
^{*}corresponding author; phone: (773)508-3756; email: gmoran3@luc.edu

Abstract

Dihydropyrimidine dehydrogenase (DPD) is a complex enzyme that reduces the 5,6-vinylic bond of pyrimidines, uracil and thymine. 5-Fluorouracil (5FU) is also a substrate for DPD and a common chemotherapeutic agent used to treat numerous cancers. Reduction of 5FU to 5-fluoro-5,6-dihydrouracil negates its toxicity and efficacy. Patients with high DPD activity levels typically have poor outcomes when treated with 5FU. DPD is thus a central mitigating factor in the treatment of a variety of cancers. 5-Ethynyluracil (5EU) covalently inactivates DPD by crosslinking with the active site general acid cysteine in the pyrimidine binding site. This reaction is dependent on the simultaneous binding of 5EU and NADPH. This ternary complex induces DPD to become activated by taking up two electrons from the NADPH. The covalent inactivation of DPD by 5EU occurs concomitantly with this reductive activation with a rate constant of $^{\sim}0.2$ s⁻¹. This k_{inact} value is correlated with the rate of reduction of one of the two flavin cofactors and localization of a mobile loop in the pyrimidine active site that places the cysteine that serves as the general acid in catalysis proximal to the 5EU ethynyl group. Efficient crosslinking is reliant on enzyme activation, but this process appears to also have a conformational aspect in that non-reductive NADPH analogues can also induce partial inactivation. Crosslinking then severs the protoncoupled electron transfer mechanism that transmits electrons 56 Å across the protein and renders DPD inactive.

Introduction

Dihydropyrimidine dehydrogenase (DPD) catalyzes the first step in the catabolic pathway for the bases, thymine and uracil. The reaction catalyzed is two-electron reduction of the 5,6-vinylic bond of the pyrimidine substrate with electrons derived from NADPH. Such reactions are often catalyzed by flavoproteins that utilize a ping pong mechanism with an intervening reduced state of the flavin ¹⁻³. Indeed, Class 1 dihydroorotate dehydrogenases catalyze ostensibly the same chemistry using such a mechanism ⁴⁻⁶. X-ray crystal structures of DPD reveal a seemingly unnecessarily complex architecture. DPD has two active sites each occupied by a flavin, one FAD and one FMN, that are separated by 52 Å and are bridged by a "wire" of four Fe₄S₄ centers. The FAD site interacts with NADP(H) molecules and the FMN site with pyrimidines (Scheme 1). The two Fe₄S₄ centers proximal to the FMN cofactor are derived from the adjacent subunit in the obligate head-to-head oriented homodimer of 113 kDa protomers interlinked by a ~10,800 Å² interface ⁷⁻⁹.



Scheme 1

DPD has considerable clinical significance. The activity of DPD is the primary means of detoxification of 5-fluorouracil (5FU), one of the most highly prescribed chemotherapeutic

agents that is used to treat a variety of cancers 10-12 (Scheme 1). Some part of the cytotoxicity of 5FU is as a disruptor of nucleic acid metabolism via its incorporation into DNA and RNA. However, the majority of 5FU toxicity arises from being metabolized to 5-FdUMP, a potent inhibitor of thymidylate synthase (TS) ¹³. Inhibition of TS reduces the cellular supply of thymidylate, thereby hindering DNA replication; 5FU is therefore particularly toxic to rapidly dividing cells. However, 5FU is a substrate for DPD, and is typically reduced and detoxified within 30 minutes of administration, undermining the efficacy arising from sustained toxicity ¹². The solution has been to administer 5FU over a period of several days via an ambulatory pump coupled to a central venous catheter ^{14, 15}. Patient variability for net DPD activity also complicates dosing of 5FU. Patients exhibit a 30-fold variation in total DPD activity, dictating that dosing, as defined by the standard of care formula, results in a spectrum of responses ranging from very little toxicity and poorer outcomes, to efficacious toxicity or extremely high toxicity that can be fatal ¹⁶⁻¹⁸. Inhibition of DPD has long been recognized as a means to eliminate dosing uncertainty. Moreover, the extended pharmacokinetic half-life would potentially allow the use of oral forms of 5FU, such as capecitabine, simplifying administration, lowering the financial burden and increasing compliance 19-23.

5-Ethynyluracil (5EU, eniluracil) is an analogue of uracil with an alkyne moiety substituent at the 5-carbon (Scheme 1). The potential of 5EU to increase efficacy of 5FU by DPD inactivation was first realized in the early 1990s. It was shown that 5EU treatment of mice and rats could induce a linear 5FU dose to plasma concentration relationship by significantly prolonging the *in vivo* half-life of 5FU. This resulted in a 2- to 4-fold increase in the observed therapeutic index ^{24,} ²⁵. Soon after, clinical trials and ensuing research articles examined 5EU as a potential adjunct

chemotherapy agent ^{26, 27} along with consideration of the possibility of co-administration with oral 5FU-derivatives that have fewer complications in administration and higher rates of compliance ²⁸⁻³³. In these studies, it was shown that in the presence of 5EU, 80% of the administered 5FU was excreted unchanged in the urine, in contrast to the >80% detoxified by DPD in untreated patients ²³. These studies also quantified the return of DPD activity post 5EU treatment and observed an increase from 2-25% of baseline over a period of 20 days, though later studies indicated a return to baseline activity within 6 days ³⁴. For either case, these data indicated that 5EU produced a profound and lasting suppression of the net DPD activity that spans the period of target 5FU toxicity ³⁰.

In clinical trials, 5EU has been shown to inhibit DPD activity and thereby sustain elevated 5FU concentrations *in vivo* ²⁹⁻³². Despite subsequent FDA approval with orphan drug status, 5EU has not yet been widely incorporated into the standard of care in clinical cancer facilities. The reason for this appears to be the lack of added benefit observed with the adopted administration strategies in conjunction with 5FU. Ten phase I and II clinical trials have evaluated the therapeutic value of 5EU. Summations of these findings suggest that the greatest benefit bestowed by 5EU co-administration is compliance in that orally available forms of 5FU are preferred by most patients ^{21, 22, 35, 36}. The lack of benefit designation was a stipulation of the FDA Oncologic Drugs Advisory Committee that roughly coincided with the discovery and adoption of alternative chemotherapies co-administered with 5FU such as irinotecan ³⁷⁻⁴⁰. The reasons underlying why no added benefit was observed when 5EU is used in combination with 5FU continue to be analyzed and discussed ^{21, 41}. One possibility is that in the majority of clinical trials the quantity of 5EU administered greatly exceeded what is required to inhibit DPD and may have encouraged

off-target covalent interactions that complicated the therapy and/or diminished the efficacy of 5FU ⁴¹. Suffice to conclude that 5EU based inhibition of DPD remains in development.

5EU was first synthesized in 1976 by Barr and coworkers with the intention that it be incorporated into nucleic acids *in vivo* in much the same manner as 5FU ⁴². Schroeder et al. later recognized the capacity for thiol-specific alkylation of the ethynyl group at the 5-position of uracil ⁴³. However, it was Porter et al. that first identified 5EU as an inactivator of dihydropyrimidine dehydrogenase, identifying a conserved active site cysteine residue as the site of covalency in the bovine form of the enzyme ⁴⁴. When structures of porcine DPD later became available, the cysteine residue in question was observed to be the candidate general acid (C671 in porcine DPD) required to supply a proton to the 5-position during reduction of the pyrimidine at the FMN active site ⁷⁻⁹. Collectively, these observations established that the mode of inhibition of DPD by 5EU was to bind in the site normally occupied by the pyrimidine substrate and cross-link with the active site cysteine general acid. This alteration potentially both occludes access to the pyrimidine binding site and severs the capacity to couple the movement of electrons and protons during catalysis.

The detailed kinetics and X-ray crystal structure of 5EU interacting with DPD have not been published. The 1992 Porter et al. study defined much of what is currently understood of 5EU's interaction with DPD 44 . This study measured a k_{inact} value and definitively identified the cysteine residue modified by 5EU during inactivation. Here we present the direct observation of the inhibition of DPD by 5EU. We have observed that 5EU inhibition occurs concomitantly with reduction of DPD by NADPH. Despite that thiol-yne covalent cross-linking does not require an external source of electrons, covalent linkage of 5EU to the active site catalytic cysteine is directly

linked to the two-electron reduction of the enzyme. In a series of inhibition trials with 5EU and NADP analogues, complete inactivation of DPD was observed only in the presence of NADPH. The net changes in the absorption spectrum of DPD during crosslinking suggest that the electrons added from NADPH reside on one of the two flavin cofactors. Our data indicates that two-electron reductive activation of DPD is required for crosslinking as this process induces a conformational change that places the active site cysteine acid adjacent to the 5EU alkyne group. Three X-ray crystal structures were solved that together describe the sequence of steps required for inactivation, define the orientation of 5EU in the pyrimidine active site and establish the dominant position of crosslinking.

Materials and Methods

Materials and Quantitation: Uracil, thymine, dimethyl sulfoxide (DMSO, & D₆-DMSO), iron (II) sulfate (FeSO₄), disodium sulfate (Na₂SO₄), sodium dithionite (Na₂O₄S₂), glycerol, and isopropylβ-D-1-thiogalactopyranoside (IPTG) were purchased from Acros Organics. Oxidized nicotinamide adenine dinucleotide phosphate (NADP+) was obtained from Alfa Aesar while the reduced form (NADPH) was obtained from Amresco. Lysogeny Broth (LB) agar tablets were bought from Bio 101, Inc. Sodium chloride (NaCl), ethylenediaminetetraacetic acid (EDTA), ampicillin, diammonium sulfate $((NH_4)_2SO_4)$, sodium citrate dihydrate (NaCT), HEPES, tri(hydroxymethyl)aminomethane (Tris) were purchased from Fischer Scientific. The plasmids used for expression of DPD wild type and variants were obtained from Genscript, and competent BL21(DE3) cells were obtained from New England BioLabs. Dibasic potassium phosphate (K₂HPO₄) and glucose oxidase were purchased from Millipore/Sigma Corp. The Miller formulation of lysogeny broth powder (LB), dithiothreitol (DTT), and flavin adenine dinucleotide (FAD) were obtained from Research Products International. Dextrose (D-glucose) was purchased from Spectrum Chemical. 5-Ethynyluracil and flavin mononucleotide (FMN) were obtained from TCI America. 6-Dihydro-NADP (6DHNADP) was prepared as previously described ⁴⁵.

Concentrations of DPD substrates and products were determined spectrophotometrically using the following extinction coefficients (NADPH; ε_{340} = 6,220 M⁻¹cm⁻¹, NADP⁺; ε_{260} = 17,800 M⁻¹cm⁻¹, uracil; ε_{260} = 8,200 M⁻¹cm⁻¹, thymine; ε_{264} = 7,860 M⁻¹cm⁻¹). The extinction coefficient used to quantify all forms of DPD was ε_{426} = 75,000 M⁻¹cm⁻¹ ⁴⁶. All concentrations indicated are post-mixing.

Expression and purification of DPD wild type and variants: Purification of porcine recombinant DPD and its variant forms was based on previous methods with alterations made to improve yield ⁴⁶⁻⁴⁸. The DPD expression plasmid, pSsDPD, was transformed into BL21(DE3) E. coli and stored at -80 °C from early log phase LB cultures as 20% glycerol stocks. For expression, cell stocks were thawed and spread (100 μL/plate) onto LB agar with 100 μg/mL ampicillin selection and grown at 37 °C for 16 hours. Cell lawns were resuspended into sterile LB broth and added to bulk LB media with 100 μg/mL ampicillin and grown at 37 °C with shaking (220 rpm) to an optical density of ~0.5 at 600 nm. The temperature was then lowered to 30 °C for an hour before the introduction of 200 μM FeSO₄ and 1 mM Na₂SO₄ to the media. IPTG (100 μM final) was then added and the culture was incubated with shaking for an additional 20 hours. Cells were harvested and resuspended in 30 mM Tris buffer, 1 mM EDTA, and 2 mM DTT, pH 8.0 (equilibration buffer) with 50 μM of both FAD and FMN added. Cells were sonicated on ice, and the cell debris was removed by centrifugation at 10,000 g for 45 min. The supernatant was then collected and brought to 35% (NH₄)₂SO₄ saturation before centrifuging at 10,000 g for 15 min. The resulting supernatant was then brought to 55% (NH₄)₂SO₄ saturation before centrifuging at 10,000 g for 15 min. The pellet was then resuspended in a quantity of equilibration buffer sufficient to bring the conductivity to <5 mS/cm before loading onto a preequilibrated Q-Sepharose anion exchange column connected to a Bio-Rad NGC FPLC system. A gradient to 300 mM NaCl in equilibration buffer was used to fractionate and elute bound proteins. Individual 5 mL fractions were assayed for activity before pooling the enzyme. The pooled enzyme was then concentrated to approximately ~2 mL and loaded onto a 26 x 1000 mm Sephacryl S-200 size exclusion column preequilibrated with 30 mM K₂HPO₄, 2 mM DTT, pH 7.4 (reaction buffer). The

protein was eluted with reaction buffer and 5 mL fractions were collected. SDS-PAGE was used to assess purity and identify fractions to combine for storage. DPD samples were tested for activity and concentrated before storing at -80 $^{\circ}$ C as ~100 μ L aliquots.

Determination of 5EU extinction coefficient: The extinction coefficient for 5EU was determined by NMR using an internal standard of known concentration. Solutions of 5EU and thymine (~20 mM) were prepared separately in D_6 -DMSO and the absorption spectrum of each was collected using a Shimadzu UV-2600 spectrophotometer. The concentration of the thymine was determined using its known extinction coefficient (ε_{265} = 7,680 M⁻¹cm⁻¹). ¹H NMR spectra in D_6 -DMSO were collected separately for the 5EU and thymine solutions. The 5EU and thymine samples were then combined in equal volume and the ¹H NMR spectrum of the mixture was recorded. The concentration of 5EU was then derived using thymine as the internal standard. The per-proton integration ratio for thymine in relation to that of 5EU was used to calculate the 5EU concentration and obtain its extinction coefficient spectrum.

Dissociation constant for WT and Cys671Ser variant DPD•pyrimidine complexes: Binding isotherms for DPD•pyrimidine complexes were based on equilibrium perturbation of the absorption spectrum of DPD. Dissociation constant measurements were carried out at 20 °C in reaction buffer. DPD was titrated with ligand and an absorption spectrum (250 to 850 nm) was recorded for each addition of pyrimidine. Spectra were corrected for dilution and the fractional change in absorption at wavelengths where perturbation was largest were used as a measure of the DPD•pyrimidine complex ([DPD•Pyr]) concentration. The changes in absorption were fit to

the quadratic form of the single site binding equation (Equation 1) in which [DPD] is the DPD concentration, [Pyr] is the pyrimidine concentration, and K_{Pyr} is the dissociation constant of the DPD•Pyr complex.

Equation 1
$$[DPD \bullet Pyr] = \frac{\left([Pyr] + [DPD] + K_{Pyr} \right) - \sqrt{\left([Pyr] + [DPD] + K_{Pyr} \right)^2 - 4([Pyr] + [DPD])}}{2}$$

DPD activity assay: Steady-state assays were used to determine the activity specific to DPD in crude and purified samples. DPD was added to a quartz cuvette containing reaction buffer with 200 μ M NADPH. The reaction was monitored at 340 nm for ~100 seconds to assess the background rate of NADPH oxidation ($\Delta \varepsilon = 6,220 \, \text{M}^{-1} \, \text{cm}^{-1}$) that arises either from the activity of contaminant proteins and/or from the futile reduction of dioxygen ⁴⁹. After the period of background rate assessment, 100 μ M uracil was added and the reaction was monitored for a further 100 seconds. The rate attributed to DPD was the difference of the two rates measured.

Michaelis-Menten analysis of the DPD Cys671Ser variant that reduces 5EU as a substrate was carried out in reaction buffer at 20 °C under anaerobic conditions using the double mixing mode of a Hi-Tech stopped-flow spectrophotometer (TgK Scientific). The enzyme was prepared anaerobically in a tonometer by exchanging argon for dissolved oxygen using a Schlenk line. The sample was subject to 30 alternating cycles of vacuum and argon gas with gentle agitation of the sample after each set of 3 cycles to promote exchange of dissolved gases. Once anaerobic, 2 U/mL glucose oxidase was added from the tonometer side arm. Substrate solutions were prepared in glass syringes. After the addition of 1 mM glucose the solutions were depleted of oxygen by inverting and sparging with argon gas for 5 minutes. After sparging 2 U/mL of glucose

oxidase was added and the sample was mounted onto the stopped-flow system 50 . For each assay the final concentrations were as follows, 1.96 μ M DPD was mixed with varied concentrations of 5EU (0.24-128 μ M) aged for 0.01 seconds, mixed with 250 μ M NADPH and the reaction was monitored at 340 nm. Initial rates were determined from the first 50 seconds of turnover by fitting to a straight line. The observed reaction rates (ν) were then plotted against the 5EU concentration and fit to the Michaelis-Menten equation (Equation 2)

Equation 2
$$\frac{v}{e} = \frac{k_{cat}[S]}{K_m + [S]}$$

Anaerobic methods for transient-state observations: Transient-state inactivation measurements were made using a stopped-flow spectrophotometer. Experiments used either single mixing (1:1) or double mixing ((1:1):1) sequences. All transient-state observations were made under anaerobic conditions. The enzyme and substrate solutions were prepared anaerobically as described above. The sample chambers of the stopped-flow instrument were filled with an oxygen reactive solution for a minimum 3 hours prior to experiments. This solution, 30 mM KPi, 1 mM glucose pH 7.5, was added to the main chamber of the tonometer and was prepared anaerobically as described above. Once anaerobic, 2 U/mL glucose oxidase was added from the tonometer side arm and the solution was introduced to the instrument to remove any residual dioxygen.

Measurement of the rate constant for DPD inactivation by 5EU: The rate constant associated with inactivation of DPD by 5EU was measured in 30 mM K₂HPO₄, pH 7.4. The reductant DTT was removed to avoid the potential for 5EU inactivation that was induced by adventitious reduction. The residual activity of DPD (2 μM) was measured after the enzyme was mixed either with 5EU (200 μ M) or 5EU and NADPH (200 and 100 μ M respectively) and aged prior to the addition of native substrates, uracil and NADPH. The enzyme and substrate solutions were prepared anaerobically as described above. Double mixing stopped-flow was used to initially age the reaction for a specified period and then mixed with saturating uracil (100 μM) and NADPH (100 μM) to observe residual activity based on the oxidation of NADPH at 340 nm. The steady-state rate data for individual age-times were fit to straight lines based on the initial rate of turnover measured from 5-10 seconds after the second mix (that introduced saturating concentrations of substrates). Initial uninhibited activity (100% activity) was based on an age-time of 0.01 seconds. The percent residual activity was plotted against the age-time and the data were fit to a single exponential according to Equation 3 to define the rate constant for inactivation. In this equation, k_{inact} is the rate constant, %Act. is the residual activity, Δ %Act. is percent inactivation, t is time, and C is the percent residual activity at infinite time.

Equation 3
$$\% Act. = \Delta \% Act. (e^{-k_{inact}t}) + C$$

The influence of NADP binding on 5EU Inactivation: The effect of NADP analogue binding at the FAD site on DPD inactivation by 5EU was tested by incubation of the enzyme with the inhibitor and an NADP analogue followed by assessment of residual activity. For each analogue, a sample

of 50 μ M DPD was divided in two and one of the samples was incubated with 2 mM 5EU and 1 mM of either NADPH, NADP+ or 6DHNADP for ~5 min at 4°C. The untreated sample was kept as an activity control. After 5 minutes, ligands were removed by a ~40,000-fold buffer exchange using 15 mL Amicon centrifugal 10 kDa nominal molecular weight cutoff filters. The untreated control samples were subject to an equal number of buffer exchange cycles. The treated and untreated samples were then assayed for activity as described above with native substrates, NADPH and uracil. Control samples were also assayed before incubation to determine initial activity to correct for activity loss was a result of mechanical handling during buffer exchanges.

Transient-state measurement of NADPH oxidation associated with 5EU inactivation: The rate constant and approximate stoichiometry for 5EU-dependent oxidation of NADPH was measured by mixing DPD with 5EU and NADPH and observing the oxidation of NADPH at 340 nm under anaerobic conditions. Individual DPD samples were made anaerobic by adding concentrated (392 μ M) aerobic enzyme to buffer pre-sparged with purified argon in the presence of the glucose/glucose oxidase scrubbing system described above. DPD (2.5, 5, 10, 20 μ M final) was mixed with 100 μ M 5EU and 50 μ M NADPH under anaerobic conditions. The data were fit to an exponential plus a straight line according to Equation 4 to obtain both an estimate of the NADPH oxidation rate constant and the amplitude of the exponential phase as a measure of the concentration of NADPH consumed. The straight-line term was included to account for an apparent non-catalytic NADPH oxidation/DPD reduction that occurs after the initial exponential process ⁴⁹. The terms in Equation 4 are: Abs_{340} ; the absorbance at 340 nm, ΔAbs_{340} ; the amplitude of the absorbance change at 340 nm, k_{obs} ; the observed rate constant, m; the slope of the line

for non-catalytic NADPH oxidation, t; time, and C; the absorbance value at infinite time for the exponential phase.

Equation 4
$$Abs_{340} = \Delta Abs_{340}(e^{-k_{obs}t}) + mt + C$$

The net absorption changes associated with the 5EU/NADPH-dependent inactivation of DPD were observed using a charge-coupled device (CCD) detector connected to the stopped-flow system in single-mixing mode. A tonometer containing 5.6 μ M DPD was made anaerobic and mixed with 100 μ M NADPH and 200 μ M 5EU, and the resulting changes were monitored for 60 seconds. The net absorption change spectrum was obtained by subtracting the CCD spectra acquired at 50 seconds from that acquired at 1.0 second. Absorption traces at 340 and 463 nm were extracted from the CCD spectral data set and fit to Equation 5 that describes a single exponential phase. In the general form of this equation, k_{obs} is the observed rate constant, Abs_X is the absorbance at wavelength X, ΔAbs_X change in absorption at wavelength X, t is time, and t0 is the absorbance value at infinite time.

Equation 5
$$Abs_X = \Delta Abs_X(e^{-k_{obs}t}) + C$$

Crystallization and structure determination of DPD•5EU complexes: Structures representing the stages of DPD inactivation were captured using X-ray crystallography. In each case, DPD crystals were grown and harvested in the dark to prevent photo-degradation of the somewhat labile FMN cofactor⁵¹.

The DPD•5EU_{open} complex was obtained by co-crystallization using the hanging drop, vapor diffusion method. Drops were formed by a variation of the reported conditions of Dobritzsch et al., by mixing 3 μL of 39 μM of DPD, 1 mM 5EU, 1 mM NADPH in 25 mM HEPES, 10 mM DTT, 10% glycerol pH 7.5 with 3 μL of well solution (1 mL) containing 50-200 mM NaCl, 19% PEG 6000, 1 mM DTT pH 4.8 g. Rectangular hexahedron crystals grew in ~16-20 hours to a size of approximately 50 x 200 x 20 μm. Crystals were cryo-protected for data collection by mounting in a loop and soaking briefly in a solution containing 100 mM NaCl, 19% PEG 6000, 20% glycerol, 1 mM DTT pH 4.8. Mounted crystals were then frozen by plunging into liquid nitrogen. Monochromatic X-ray diffraction data were collected at the Life Science Collaborative Access Team LS-CAT beamline 21-ID-D at the Advanced Photon Source at Argonne National Laboratory. Data were collected at a wavelength of 1.127 Å and a temperature of 100 K using a Dectris Eiger 9M detector. Data sets were processed and analyzed with Xia2 software^{52, 53}. Data processing statistics are given in Table 1.

The DPD•5EU•NADP(H)_{closed} and DPD-5EU•NADP(H)_{covalent} complexes were obtained by soaking. In each case DPD was crystallized by the vapor diffusion, hanging drop method by mixing 3 μL of 39 μM DPD in 25 mM HEPES, 2 mM DTT, 10% glycerol, pH 7.5 with 3 μL of well solution containing 100 mM NaCl, 2 mM DTT, 18% PEG 6000, pH 4.7. Rectangular hexahedron crystals grew in ~16-20 hours to a size of approximately 50 x 200 x 20 μm. For the DPD•5EU•NADP(H)_{closed} complex the crystals were soaked for 20 minutes in 25 mM HEPES, 100 mM NaCl, 2 mM DTT, 100 μM NADPH, 100 μM 5EU, 20% PEG 6000, 20% PEG 400, pH 7.5. Crystals were then frozen by plunging into liquid nitrogen. To obtain the DPD-5EU•NADP(H)_{covalent} complex, the wells containing the crystals were made anaerobic by an addition of Na₂S₂O₄ to 10 mM and re-sealed

with the cover slide before transfer to a Plas-Labs 830 series glove box housing a Motic binocular microscope coupled to a Accu-Scope Excelis 1080P camera projecting images to an 11.6 inch HD monitor. The glove box atmosphere was depleted of dioxygen by flushing with nitrogen gas. Total oxygen partial pressure inside the glove box was at most 0.4% during crystal handling. The crystals were soaked for 2 hours in 25 mM HEPES, 100 mM NaCl, 2 mM DTT, 100 μM NADPH, 100 μM 5EU, 20% PEG 6000, 20% PEG 400, pH 7.5 and then frozen in liquid nitrogen before being removed from the glove box. Diffraction data for the DPD•5EU•NADP(H)_{closed} and DPD-5EU•NADP(H)_{covalent} complexes were collected at 100 K at the Life Science Collaborative Access Team (LS-CAT) beamline 21-ID-D of the Advanced Photon Source at Argonne National Laboratory. The beamline was equipped with a Dectris Eiger 9M detector. The wavelength was fixed at 0.97856 Å. Data sets were processed and analyzed with Xia2 software, data processing statistics are given in Table 1.

Model Building and Refinement: The DPD structure was solved by molecular replacement using PHASER in Phenix^{54, 55}. The starting search model was the previously published structure of DPD (PDB code: 1H7X). The model building and refinement were accomplished in $Coot^{56}$ and Phenix, respectively, as an iterative process until the lowest possible R_{free}/R factor values were attained. Structural depiction figures were prepared from the model and omit density maps that were derived from removing 5EU, FMN, FAD, NADPH and Cys671 before being rendered in PyMol (Schrödinger Software).

Complex	DPD•5EU _{open}	DPD•5EU•NADP(H)closed	DPD-5EU•NADP(H)covalent
PDB code	7LJS	7LJT	7LJU
Space group	P 1 2 ₁ 1	P 1 2 ₁ 1	P 1 2 ₁ 1
Unit Cell dimension			
α, β, γ (deg)	90, 95.95, 90	90, 95.71, 90	90, 96.03, 90
a, b, c (Å)	82.0, 160.0, 164.1	82.2, 158.9,162.1	82.1, 158.9, 163.2
Processed Resolution (Å)	2.00	1.98	1.87
R _{merge} a (%)	17.2 (86.9)	13.8 (81.5)	21.5 (106.6)
R _{pim} ^c (%)	12.1 (66.5)	7.4 (45.5)	11.7 (66.8)
Ι/σ (Ι)	5.6 (1.1)	7.6 (1.6)	6.30 (1.10)
CC ½ d (%)	99.2 (37.7)	98.9 (61.5)	98.9 (52.0)
Completeness (%)	90.2(66.0)	88.6 (77.0)	98.3 (92.4)
Multiplicity	2.9 (2.1)	4.2 (4.0)	4.1 (3.4)
No. Reflections	747583	1065501	1387185
No. Unique Reflections	255614	254113	336013
		Refinement	
R _{work} e/R _{free} f (%)	17.21/22.86	18.30/21.90	17.19/21.09
No. of Atoms			
protein	30857	30847	30773
ligand	504	696	708
water	2171	3560	3389
		rage B factors (Ų)	
protein	30.16	20.39	26.33
		RMSD ^g	
bond lengths (Å)	0.036	0.009	0.010
bond angles (deg)	2.32	1.10	1.22
	Rama	achandran plot (%)	
favored	94.84	95.44	96.25
allowed	4.34	4.02	3.35
outliers	0.82	0.54	0.40

 $[^]aR_{merge} = \Sigma |I_{obs} - I_{avg}|/\Sigma I_{avg}$, $^bThe values for the highest-resolution bin are in parentheses, <math>^cPrecision-indicating merging R$, $^dPearson correlation coefficient of two "half" data sets, <math>^eR_{work} = \Sigma |F_{obs} - F_{calc}|/\Sigma F_{obs}$, $^fFive percent of the reflection data were selected at random as a test set, and only these data were used to calculate <math>R_{free}$, gRoot -mean square deviation.

Table 1. Crystallographic data collection and model refinement statistics for the DPD•5EU complexes.

Results

Dissociation constant for the DPD•5EU complex: The concentration of 5EU was defined using the extinction coefficient ε_{285} = 4,340 M⁻¹cm⁻¹ that was measured by ¹H NMR integrations in the presence of an internal standard of known absorptivity (Figure 1A). In the absence of NADPH, 5EU associates with DPD to form an equilibrium concentration of the DPD•5EU complex. The association of 5EU perturbs the enzyme spectrum permitting sequential titration and determination of the binding equilibrium constant (Figure 1B). The changes in absorbance at the maximally perturbed transition (497 nm) were plotted against the 5EU concentration and fit to determine a dissociation constant of 9.5 \pm 1.2 μ M. Curvature in the isotherm is indicative of equilibrium binding and not stoichiometric covalent inactivation, indicating that 5EU alone is insufficient to inhibit the resting, non-activated form of DPD.

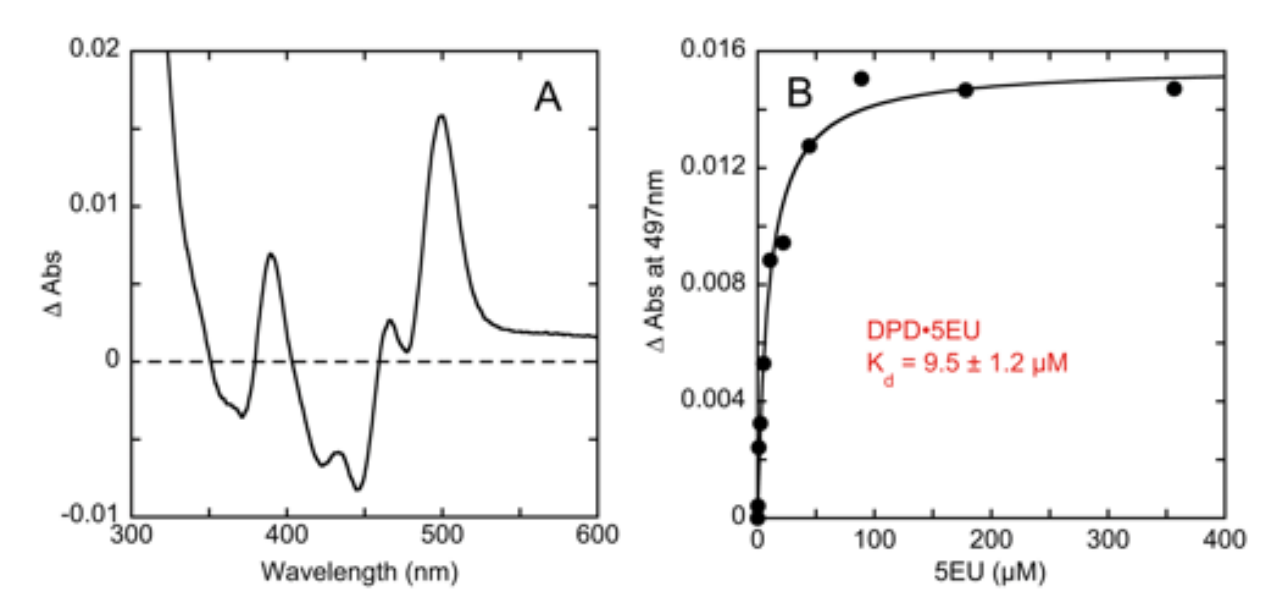


Figure 1. Determination of the DPD \bullet 5EU complex dissociation constant. A. The difference spectrum observed when 6.2 μ M DPD was mixed with 100 μ M 5EU. B. The ligand binding isotherm for 7.6 μ M DPD titrated with 5EU (0.34-356 μ M) fit to the quadratic form of the single site binding equation (Equation 1).

Measurement of the rate constant for DPD inactivation by 5EU: The rate constant for bovine DPD inactivation by 5EU has been previously reported by Porter et al., as $0.30 \pm 0.03 \, \text{s}^{-1.44}$. This measurement was made by 5EU titration in the presence of NADPH and absence of a substrate pyrimidine and so was a composite measurement that was influenced both by 5EU binding and the rate constant for inactivation. Though not stated, presumably these prior measurements were made by manual mixing, as the earliest measurement in these experiments corresponded to ~5 seconds. We measured the rate constant for inactivation by double mixing stopped-flow methods which provided both considerably higher time resolution and access to earlier incubation times. Porcine DPD was combined with saturating 5EU in the presence or absence of NADPH, aged for a specific time and then mixed with saturating concentrations of NADPH and uracil (Figure 2). The residual activity was measured by fitting the initial rate of the observed steady-state trace. This value was plotted against the age-time and the data obtained were fit to Equation 3. The data indicate that rapid inactivation of DPD by 5EU occurs only in the presence of NADPH with a rate constant of 0.22 ± 0.01 s⁻¹; in excellent agreement with the prior report. When incubated in the absence of NADPH, inactivation was not observed. From these data we can conclude that inactivation of DPD by 5EU is contingent on the inclusion of NADPH and that inactivation, at least in part, takes advantage of DPD activation catalysis (see below).

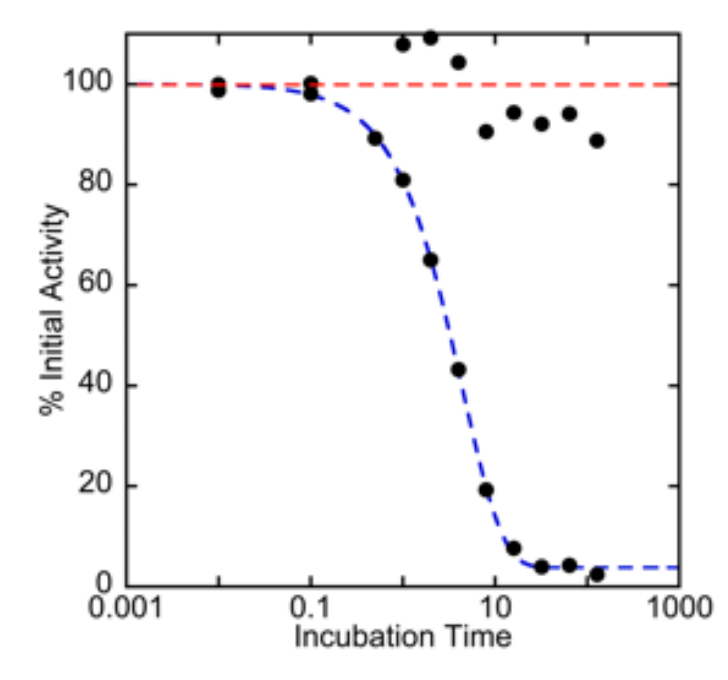


Figure 2. The rate and ligand dependence of inactivation of DPD. Circular graph markers depict the residual activity of 2 µM DPD when mixed with either 5EU (200 µM) (red dashed line) or NADPH (100 μM) and 5EU (200 μM) (blue dashed line). In each case the mixture was aged for a range of times and then mixed with 100 µM uracil and 100 µM NADPH (all concentrations post mixing) and percentage of residual activity was based on the rate of NADPH oxidation at 340 nm. The data obtained for incubation with 5EU and NADPH were fit to a single exponential according to Equation 3 to define a rate constant of 0.22 ± 0.01 s⁻¹ and 96% inactivation. The data obtained for incubation with 5EU only were assumed to indicate scatter and were described by a line that is representative of the average activity for all aged times.

The influence of NADP binding on 5EU Inactivation: The chemistry of 5EU inactivation of DPD is presumed to be that of facile thiol-yne "click" chemistry that would not require an external source of electrons to bring about a covalent association of the 5EU ethynyl group and the thiol of DPD Cys671 ⁵⁷. To establish if DPD inactivation by 5EU involves hydride transfer from NADPH or is triggered solely by NADPH binding, DPD was incubated with 5EU in the presence and absence of NADPH and NADPH-analogues that are incapable of canonical hydride transfer. These samples were then buffer exchanged to remove the ligands and tested for residual activity relative to control samples manipulated in an identical manner (Figure 3). These data show that complete inactivation of DPD occurs only in the presence of both 5EU and NADPH. Incubation with either the product, NADP* or the NADPH isomer, 6DHNADP ^{45, 58} did not result in complete DPD inactivation. However, both NADPH analogues induced fractional (~25%) inactivation compared to controls which suggests that 5EU inactivation includes a conformational component

where occupancy of the NADP binding site proximal to the FAD cofactor induces partial inactivation by 5EU, 56 Å distant at the pyrimidine binding site proximal to the FMN cofactor.

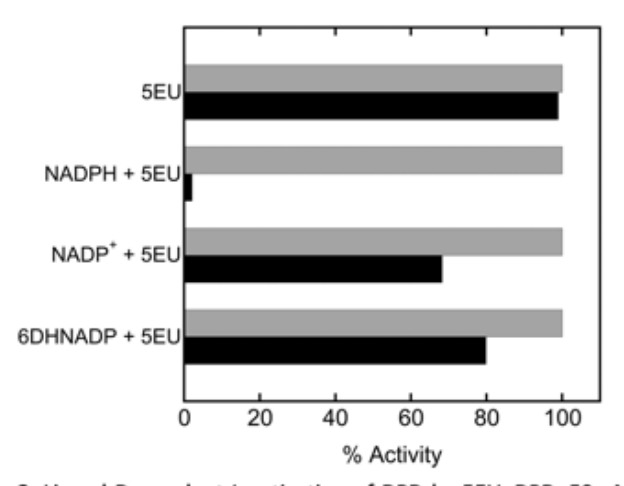


Figure 3. Ligand-Dependent Inactivation of DPD by 5EU. DPD, 50 μ M was incubated with 1 mM 5EU and 1 mM of NADPH, NADP+ or 6DHNADP for ~5 min. Non-covalently bound ligands were then removed by a 40,000-fold buffer exchange. The samples were then assayed for activity with native substrates, NADPH and uracil. Control samples (grey) were treated in an equivalent manner (without added ligands) and were also assayed before incubation to determine initial activity to establish if activity loss was a result of mechanical handling during buffer exchanges. All data were normalized to the control samples to give percent activity for the 5EU treated samples (black).

Transient-state measurements of NADPH oxidation associated with 5EU inactivation: The data in Figure 3 suggest that the oxidation state of the NADP is a primary determining factor in 5EU inactivation of DPD. To establish whether NADPH oxidation is required for 5EU crosslinking, limiting concentrations of DPD were mixed with excess 5EU and NADPH using anaerobic stopped-flow methods and the change in absorbance at 340 nm observed (Figure 4). For each concentration of DPD for which the 5EU and NADPH concentrations were approximately pseudo-first order (2.5, 5.0, $10 \mu M$ DPD) the data could be adequately described by an exponential added to a straight line according to Equation 4. This was interpreted as oxidation of NADPH that occurred with the average rate constant of 0.18 ± 0.02 s⁻¹, ostensibly coincident with the rate of 5EU crosslinking (see above). The ensuing linear decrease in absorption was assigned to slow

uncoupled reduction of DPD by NADPH. The amplitudes obtained from the fit for the exponential phase were divided by the change in extinction coefficient for the oxidation of NADPH at 340 nm (6,220 M⁻¹cm⁻¹) and plotted against the DPD concentrations. The slope of the line obtained was 0.91 consistent with ~1:1 NADPH oxidation and DPD inactivation in the exponential phase (Figure 4 inset). In our prior studies of DPD we demonstrated that concentrations of NADPH lower than the enzyme concentration induce activity in only one of the two subunits of the DPD dimer. This was ascribed to very high affinity for NADPH of the activated subunit. In this instance the excess NADPH in these reactions permits activation of both subunits and brings the observed stoichiometry for NADPH-dependent activation and DPD crosslinking close to 1:1.

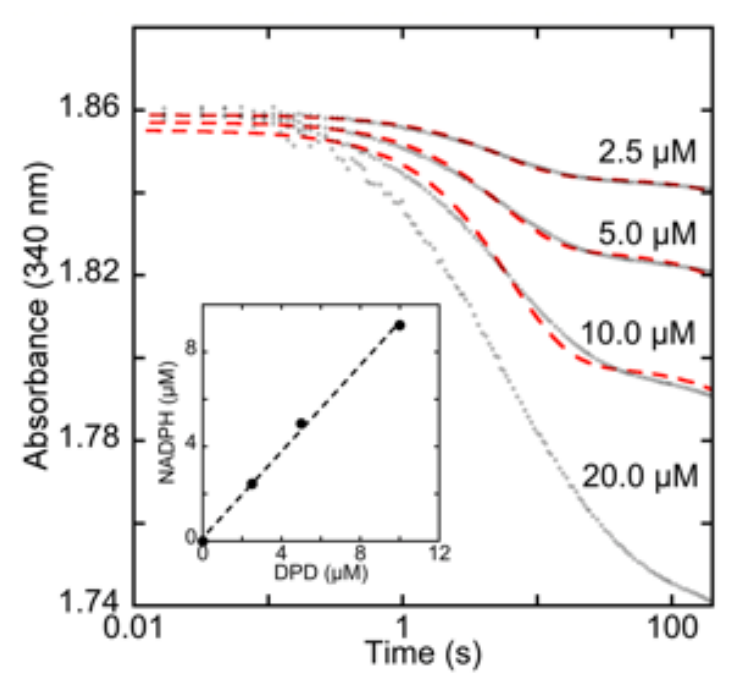


Figure 4. 5EU Dependent Oxidation of NADPH by DPD. Indicated concentrations of DPD were mixed with 50 μ M 5EU and 50 μ M NADPH under anaerobic conditions (all concentrations post mixing). The data for 2.5, 5.0, 10.0 μ M DPD were fit (red dashed line) to an exponential plus a straight line according to Equation 4 to obtain an estimate of the NADPH oxidation rate constant and the amplitude of the exponential phase as a measure of the concentration of NADPH consumed. The data indicate a average rate constant for NADPH oxidation of 0.18 \pm 0.02 s⁻¹ and the concentration of NADPH consumed is approximately equal to the DPD concentration (Inset).

Given that crosslinking of the 5EU ethynyl group with the Cys671 thiol does not require redox chemistry, it is reasonable to conclude that electrons liberated from NADPH during DPD inactivation by 5EU must remain on the enzyme. To assess this possibility spectrophotometrically, DPD was mixed under anaerobic conditions using stopped-flow with saturating concentrations of 5EU and NADPH. Spectra were recorded from 250-800 nm using a charge coupled device (CCD) detector (Figure 5). The difference spectrum obtained for this process has the shape of the changes observed during reduction of a flavin added to that observed with oxidation of NADPH (Figure 5A inset). While quite qualitative, these data suggest that the two electrons consumed to bring about 5EU crosslinking reside on the isoalloxazine of one of the two flavins of DPD. Traces for 463 nm and 340 nm extracted from the CCD dataset show the time dependence of changes that occur at these wavelengths (Figure 5B & C). These traces were fit to a single exponential expression (Equation 5) to define the rate constant and extinction coefficient changes associated with DPD inactivation. The fit of the trace for 463 nm returned a rate constant of 0.14 ± 0.01 s⁻¹ and an extinction coefficient change of 6,800 M⁻¹cm⁻¹ when divided by the DPD concentration. The fit of the trace for 340 nm gave a rate constant of 0.17 ± 0.01 s⁻¹ and an extinction coefficient change of 6,400 M⁻¹cm⁻¹ when divided by the DPD concentration. These rates are in good agreement with the inactivation rate constants measured in other experiments of this study and the changes in absorptivity are respectively consistent with reduction of a single flavin and oxidation of NADPH.

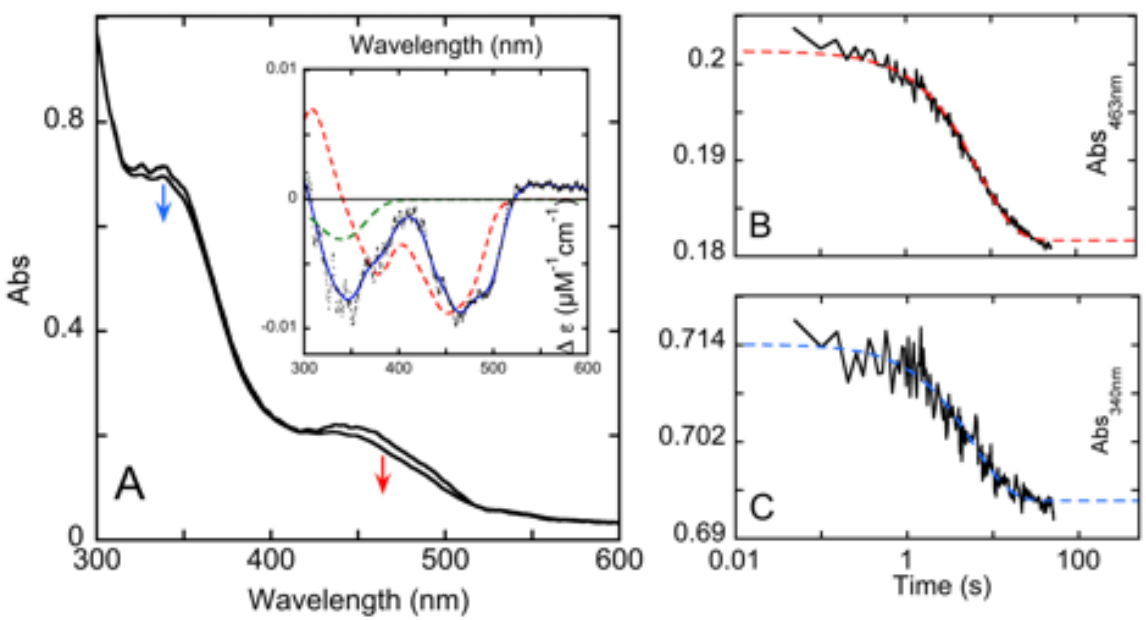


Figure 5. Spectrophotometric evidence that electrons taken up during SEU-dependent inactivation of DPD from NADPH reside on a flavin cofactor. **A.** Shown at left are the spectra recorded at 1.0 and 50.6 seconds when 2.8 μ M DPD was reacted with 200 μ M 5EU and 100 μ M NADPH under anaerobic conditions. Inset shows the difference of these two spectra fit to an interpolated line (blue line) and overlaid with the difference spectra for flavin reduction (red dashed line) and NADPH oxidation (green dashed line). **B.** The extracted trace for data collected at 340 nm fit to one exponential according to Equation 5 to yield a rate constant of 0.17 \pm 0.01 s⁻¹. The observed amplitude at 340 nm is consistent with 2.8 μ M NADPH consumption. **C.** The extracted trace at 463 nm was fit to Equation 5 to a rate constant of 0.14 \pm 0.01 s⁻¹.

The interaction of 5EU with the Cys671Ser variant. As a proof of concept, 5EU was reacted with the Cys671Ser variant of DPD. The hydroxyl general acid available in this variant is inherently less reactive with the ethynyl group of 5EU and so is not crosslinked. As such 5EU is observed to be a substrate for this form of DPD and associates with a similar dissociation constant to that observed with the wild-type enzyme (Figure 1 ca. 6) The Cys671Ser variant has a turnover number 100-fold slower than that observed for the wild-type enzyme with uracil. Interestingly the rate of turnover of this variant with 5EU is similar to the rate observed with uracil and 35-fold more rapid than is observed with thymine ⁴⁹. These data indicate that volume of the pyrimidine 5-substituent has influence but is not the only determinant of the rate of turnover. Our prior studies have indicated that availability of the proton from cysteine (or serine) in the 671 position defines the rate of turnover and that this number is not correlated with the pKa difference for cysteine and serine

residues ⁴⁹. This is in contrast to observations made with dihydroorotate dehydrogenase where substitution of the active site cysteine acid with serine resulted in a rate of hydride transfer that was 10⁶-fold slower for the serine variant, roughly correlated with the difference in pKa's ⁵.

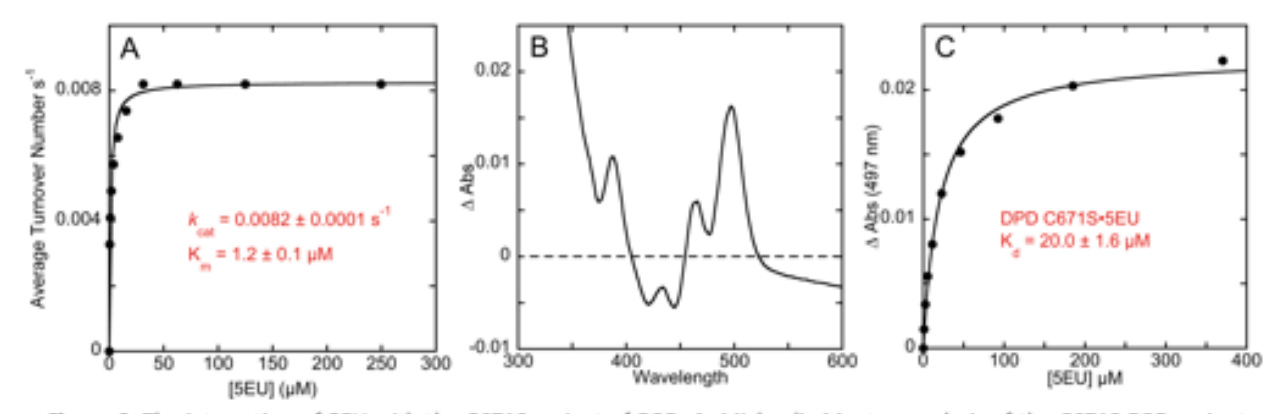


Figure 6. The interaction of 5EU with the C671S variant of DPD. A. Michaelis-Menten analysis of the C671S DPD variant. DPD, 1.96 μM, was mixed with varied (0.48-256 μM) 5EU in the presence of 250 μM NADPH and fit to the Michaelis-Menten equation (Equation 2). B. The difference spectrum observed when 4.7 μM DPD C671S was mixed with 370 μM 5EU. C. The ligand binding isotherm for 4.7 μM DPD C671S titrated with 5EU (0.36-370 μM) fit to the quadratic form of the single site binding equation (Equation 1).

Structures of DPD•5EU complexes: For the three structures of DPD presented here, one asymmetric unit is comprised of four subunits that form two DPD dimers (AB-CD). Conformational changes relevant to 5EU inhibition are observed only in subunit C, potentially indicating a role for single-site asymmetry in the mechanism and/or the possibility of accessibility artifacts arising from dimer stacking in the crystal lattice. CD-dimer asymmetry arises as a consequence of conformational changes near the pyrimidine binding site for a single loop that contains the presumed catalytic general acid Cys671. The structure of the DPD•5EU_{open} complex (PDB ID: 7LJS) was solved to a resolution of 2.00 Å and in terms of completeness is representative of the three structures presented (*see below*). This structure was obtained by soaking with both 5EU and NADPH, however, the soaking/cryo-condition used had a pH of 4.8 ensuring that all added NADPH was lost to cyclization ⁵⁹. As such the resultant complex was captured with only 5EU in the FMN active site and the loop containing Cys671 in a conformation that placed the thiol

10.5 Å from the ethynyl group of 5EU (Figure 7A). In subunit A of this structure residues 675-681 (ERGMG) and 902-907 (AAFPPL) had no discernable density and were not modeled. Similarly, in subunit B residues 674-679 (GMGERG) and 902-907 (AAFPPL) were absent from the observed density. Subunit C is missing density only for residues 676-681 (RGMG). We have recently demonstrated that the active form of DPD is the two-electron reduced state that occurs when a hydride from NADPH is transferred to the enzyme in a process stimulated by the binding of pyrimidines⁴⁹. The conformation observed in the DPD•5EU_{open} complex therefore represents the resting, non-activated form of the enzyme in complex with the 5EU inhibitor.

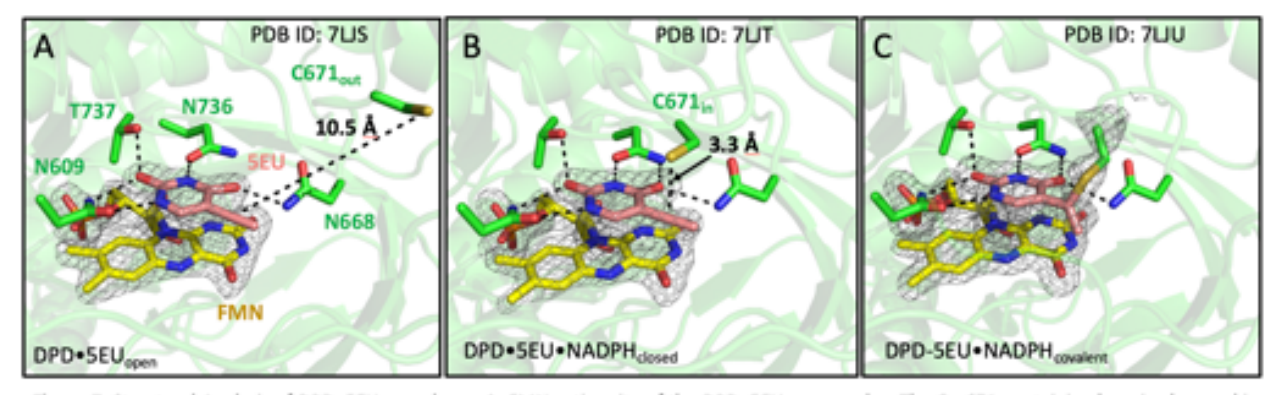


Figure 7. Structural Analysis of DPD+SEU complexes. A. FMN active site of the DPD+SEU open complex. The Cys671-containing loop is observed in the open position in the absence of NADPH at the FAD site. B. FMN site of the ternary DPD+NADP(H)+SEU complex. C. The FMN site for the crosslinked structure of DPD-SEU+NADP(H) covalent complex. All structures display omit map density for flavin and SEU contoured to 2.5 sigma and derived by omitting SEU, FMN, NADPH (when applicable), FAD and Cys671 from the model.

In the subsequent 1.98 Å resolution structure for the DPD•5EU•NADP(H)_{closed} complex (PDB ID:7LJT) the loop containing Cys671 of subunit C has a significantly changed conformation in that the thiol of Cys671 is now 3.3 Å from the proximal carbon of the 5EU ethynyl group (Figure 7B). The RMSD compared to a single subunit of the DPD•5EU_{open} complex structure for 7678 atoms was 1.567 Å, with the only significant conformational change occurring for this loop (669-684) (Figure S1). This complex formed *in crystallo* with a 20-minute soak in the presence of excess 5EU and NADPH. In this structure NADPH has been modelled into the observed density, though

the oxidation state of this ligand was not known. The basis for modelling NADPH is that the activated form of the enzyme was previously shown to exhibit exceedingly high affinity for NADPH (supplied in excess with the soaking condition)⁴⁹. It is observed that the dihydronicotinamide stacked with the isoalloxazine of the FAD cofactor such that the nicotinamide C4 is 2.8 Å from the flavin N5. In this position, the nicotinamide is localized in a region of apparent negative potential as a result of its proximity to the carboxyl groups of Asp342, Asp346, and Glu376 that are all within ~4 Å of the base (Figure S2). Selectivity for NADP(H) is evidently imparted by interactions of the substrate's 2'-phospho group with Arg364, Lys365, and Arg371. The binding of NADPH perturbs the positions of Arg364 that moves to form a charge association with NADP(H), and Asn487 that is displaced with the binding of this ligand but has no defined rotamer state when subunits are compared.

To capture the DPD-5EU•NADP(H)_{covalent} crosslinked structure (PDB ID: 7LJU), DPD was soaked with excess 5EU and NADPH under diminished oxygen atmosphere (0.1-0.4% O₂) for two hours. This structure was obtained at a resolution of 1.87 Å and exhibited similar gaps in density as defined above for the open complex. This structure clearly showed density linking the Cys671 thiol to the proximal carbon of what was the 5EU ethynyl group, consistent with Markovnikov regional selection (Figure 7C). In this structure the Cys671 loop (669-684) conformation is dramatically altered from that in the open complex (Figure S1).

These are the first DPD structures solved in complex with 5EU, an FDA approved 5FU chemotherapy sensitizer. Moreover, they represent a facsimile both the proposed normal sequence that occurs for reductive activation prior to catalysis ⁴⁹, and of the sequence of events that occur in the inactivation of DPD by 5EU. Collectively they suggest that the 5EU molecule

binds to DPD and stimulates reductive activation of the enzyme in a manner similar to that of substrate pyrimidines. Reductive activation induces a conformational change in the only significantly mobile part of the protein, the section of loop that includes the catalytic general acid Cys671. In catalysis this conformational shift places the Cys671 thiol adjacent to the pyrimidine for proton-coupled electron transfer from NADPH. However, for 5EU, this closed conformation promotes the thiol-yne reaction that results in indelible inactivation of the enzyme. As such 5EU is a mechanism-based inactivator that hijacks both the activation mechanism and the catalytic mechanism of DPD.

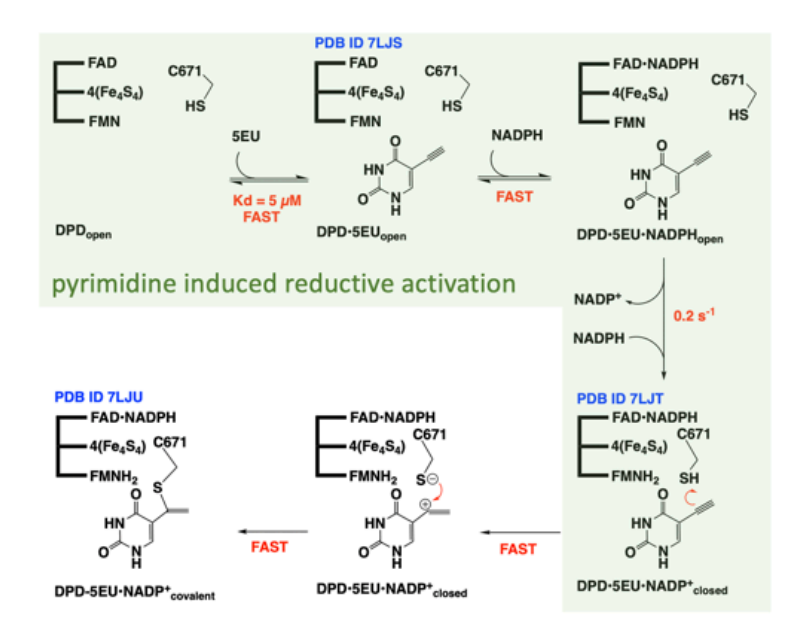
Discussion

The initial study of Porter et al. stands as the first biochemical investigation of DPD inactivation by 5EU ⁴⁴. Despite extensive investigation of the efficacy of co-administration of 5EU with 5FU, neither the detailed mechanism nor structural evidence of the interaction of 5EU with DPD has been presented. In this study we offer a comprehensive description for the events that occur during covalent modification of DPD by 5EU. The data indicate that 5EU is a mechanism based inactivator that utilizes the reductive activation mechanism of DPD to bring the alkyne and thiol moieties to within ~3 Å such that crosslinking may occur. The data show that specificity of 5EU for DPD is imparted as a consequence of 5EU inducing the reductive activation sequence in which two-electrons are acquired from NADPH in response to pyrimidine binding and that the reduced state of the enzyme exhibits a conformational bias that has the thiol of Cys671 proximal to the 5-position of the pyrimidine (Scheme 2 & Figure 7).

The pyrimidine binding site has six apparent hydrogen bonding interactions with the base (Figure 7 & Figure S1). However, neither the 6 nor the 5 position is able to be engaged in such interactions, and no voluminous residues are observed that crowd this portion of the substrate ⁸. In the absence of NADPH, 5EU is observed to bind reversibly to the DPD•5EU complex with high affinity that is only ~3-fold lower than that observed for uracil (Figure 1B). Prior studies have shown that DPD is somewhat insensitive to the volume of the substituents at the 5-position of pyrimidine substrates, consistent with the dual specificity toward uracil and thymine ^{9,60}. The added elongated volume of the 5EU methyne carbon compared to thymine does not impede binding significantly and no alterations in local structure are observed with association.

The observed rate of inactivation of DPD by 5EU is ~0.2 s⁻¹ (Figure 2). This rate is correlated with the rate constants observed for 5EU induced NADPH oxidation and concomitant flavin reduction during activation (Figures 4 & 5). These data indicate that 5EU is sufficiently similar to native substrates to act as an effector, stimulating the enzyme to activate by taking up two electrons. That crosslinking, NADPH oxidation and flavin reduction are observed to occur concomitantly indicates that the actual rate of the thiol-yne reaction is rapid relative to the rate of hydride transfer from NADPH during activation. The observed rate of activation in the presence of 5EU is ~20-fold slower than the rate with uracil or thymine indicating that the identity of the pyrimidine associated at the FMN site influences the rate of hydride transfer from NADPH, 60 Å distant at the FAD site. This apparent capacity for the ligand in one active site to influence the fate of a ligand in another was observed for non-reducing NADPH analogues that were able to induce partial crosslinking by 5EU (Figure 2). In order to establish if the structural data presented in this study had evidence of conformational communication between FAD and FMN active sites, the DPD•5EU_{open} and DPD•NADP(H)•5EU_{closed} complex structures were compared using the Structural Comparison facility in Phenix software. This analysis indicated no significant change in the position of either peptide backbone or residue side chain rotamers save for residues that comprise the mobile Cys671 loop as described.

The three structures presented in this study depict events in an apparent sequence that covalently modifies cysteine 671 of DPD rendering the enzyme inactive (Figure 7 & Scheme 2).



Scheme 2: The Proposed Chemistry of 5EU DPD Inhibition.

The only significant structural movement observed among the three structures presented occurs for the loop that spans residues 669-684 and the two states of this loop toggle the position of the Cys671 general acid by 8 Å. In one state the thiol is 10.5 Å from the proximal ethyne carbon and in the other state it is 3.3 Å from this position. As was noted previously by Porter et al., in the absence of NADPH no crosslinking with 5EU is observed (Figure 3) ⁴⁴. These data correlated with the DPD•5EU_{open} complex structure suggest that in the resting non-activated state of the enzyme, the dominant conformational state of the dynamic 669-684 loop is the open position, diminishing the opportunity for the 5EU crosslink reaction (Figure 7 & S1). The structure of the DPD•5EU•NADP(H)_{closed} complex is therefore a curiosity. In this structure the Cys671 thiol and 5EU ethynyl moiety clearly have not formed a bond and reside 3.3 Å apart. That these known reactive groups could be proximal without reacting is unexpected and suggests either that other local environmental factors influence the efficiency of the crosslinking reaction or that this reaction is impeded by the crystal lattice.

The inactivation of DPD by 5EU occurs coincident with reduction of a flavin cofactor (Figures 2, 4, 5). The DPD•5EU•NADP(H)_{closed} structure was solved from a crystal subjected to a 20 min soak at near neutral pH in the presence of 5EU and NADPH under aerobic conditions. One possible explanation is that the oxidative inactivation of the enzyme by reduction of dioxygen changed the local electrostatic environment impeding the crosslinking reaction. However, that the loop is not observed to return to the open state in all subunits of the asymmetric unit suggests that this is not the case. As such the preferred rationalization is that the crosslink forms more slowly *in crystallo*, which is supported by the fact that a two-hour soak yielded the crosslinked state.

The DPD-5EU•NADP(H)_{covalent} complex was obtained by an extended soak with 5EU and NADPH in dinitrogen atmosphere with a low partial pressure of dioxygen. These conditions were chosen to retain the oxidation state of the activated and crosslinked enzyme. In this structure the oxidation state of the flavin cofactors could not be established by configurational shape as both FAD and FMN are flat within the model angle error of this 1.87 Å resolution structure. The flat shape of the FMN, however does not define the oxidation state as this cofactor is highly crowded and may not exhibit significant pleating when reduced⁶¹.

The crosslink between 5EU and Cys671 is observed to form at the proximal carbon of the ethynyl group with respect to the pyrimidine ring defining the mode of action of the inhibitor. The events that induced this reaction are the events of activation where pyrimidine binding promotes hydride transfer from NADPH to form the two-electron reduced and activated state of the enzyme. In these *in vitro* experiments, the 5EU inhibitor is directed to react in the process of

reductive activation. However, it is as likely that the inhibitor could crosslink with pre-activated enzyme that would be expected to predominate *in vivo*.

The formation of the crosslink eliminates the active site general acid and prevents turnover. However, this linkage does not appear to prevent the movement of the 669-684 loop as uracil can be observed to bind to the 5EU inactivated enzyme with a binding constant comparable (~3-fold) to that observed with the unmodified resting enzyme (Figure S3). It therefore must be concluded that crosslinking biases the loop position to reside more often in the closed state but does not prevent movement of this loop. Moreover, it must be asserted that the position of the dynamic loop is likely not fixed at any stage of catalysis or when inhibited as the exchange of substrate and product pyrimidines would be obstructed if the closed conformation were to persist and so we conclude that activation of the enzyme moves the equilibrium position of the loop to favor the closed state in order to sustain turnover.

Conclusive Remarks

DPD nullifies 5-fluorouracil toxicity by reduction forming 5-fluoro-5,6-dihydrouracil. 5-ethynyluracil enhances 5-fluorouracil chemotoxicity by covalent modification of the active site general acid cysteine of DPD. Inactivation of DPD by 5EU is dependent on the proximity of the ethynyl group of the inhibitor and the thiol of Cys671. The resting, as isolated, state of DPD is not subject to inhibition by 5EU. Inactivation occurs concomitantly with reductive activation of the enzyme by NADPH. This activation of the enzyme biases the average position of the only dynamic region of the enzyme, the loop harboring Cys671, to a closed state that places the ethynyl and

thiol groups within 3.3 Å. The thiol-yne reaction then occurs, forming a crosslink with the proximal ethynyl carbon, indelibly inactivating the enzyme.

Supporting Information

Contents:

Figure S1. Comparison of the mobile loop positions in the DPD•5EU_{open} and DPD•5EU•NADP(H)_{closed} complexes.

Figure S2. The NADPH Binding Pose of the DPD•5EU•NADP(H)_{closed} complex.

Figure S3. The uracil binding isotherm of for DPD covalently inactivated by 5EU.

References

- [1] Stott, K., Saito, K., Thiele, D. J., and Massey, V. (1993) Old Yellow Enzyme. The discovery of multiple isozymes and a family of related proteins, *J Biol Chem 268*, 6097-6106.
- [2] Nizam, S., Gazara, R. K., Verma, S., Singh, K., and Verma, P. K. (2014) Comparative structural modeling of six old yellow enzymes (OYEs) from the necrotrophic fungus Ascochyta rabiei: insight into novel OYE classes with differences in cofactor binding, organization of active site residues and stereopreferences, *PLoS One 9*, 1-13.
- [3] Nizam, S., Verma, S., Borah, N. N., Gazara, R. K., and Verma, P. K. (2014) Comprehensive genome-wide analysis reveals different classes of enigmatic old yellow enzyme in fungi, *Sci Rep 4*, 1-11.
- [4] Fagan, R. L., Nelson, M. N., Pagano, P. M., and Palfey, B. A. (2006) Mechanism of flavin reduction in class 2 dihydroorotate dehydrogenases, *Biochemistry 45*, 14926-14932.
- [5] Fagan, R. L., Jensen, K. F., Bjornberg, O., and Palfey, B. A. (2007) Mechanism of flavin reduction in the class 1A dihydroorotate dehydrogenase from Lactococcus lactis, *Biochemistry 46*, 4028-4036.
- [6] Reis, R. A. G., Calil, F. A., Feliciano, P. R., Pinheiro, M. P., and Nonato, M. C. (2017) The dihydroorotate dehydrogenases: Past and present, *Arch Biochem Biophys* 632, 175-191.
- [7] Dobritzsch, D., Persson, K., Schneider, G., and Lindqvist, Y. (2001) Crystallization and preliminary X-ray study of pig liver dihydropyrimidine dehydrogenase, Acta Crystallogr D Biol Crystallogr 57, 153-155.

- [8] Dobritzsch, D., Schneider, G., Schnackerz, K. D., and Lindqvist, Y. (2001) Crystal structure of dihydropyrimidine dehydrogenase, a major determinant of the pharmacokinetics of the anti-cancer drug 5-fluorouracil, *EMBO J 20*, 650-660.
- [9] Dobritzsch, D., Ricagno, S., Schneider, G., Schnackerz, K. D., and Lindqvist, Y. (2002) Crystal structure of the productive ternary complex of dihydropyrimidine dehydrogenase with NADPH and 5-iodouracil. Implications for mechanism of inhibition and electron transfer, *J Biol Chem* 277, 13155-13166.
- [10] Longley, D. B., Harkin, D. P., and Johnston, P. G. (2003) 5-fluorouracil: mechanisms of action and clinical strategies, *Nat Rev Cancer 3*, 330-338.
- [11] Milano, G., and Etienne, M. C. (1994) Dihydropyrimidine dehydrogenase (DPD) and clinical pharmacology of 5-fluorouracil (review), *Anticancer Res* 14, 2295-2297.
- [12] Heggie, G. D., Sommadossi, J. P., Cross, D. S., Huster, W. J., and Diasio, R. B. (1987) Clinical pharmacokinetics of 5-fluorouracil and its metabolites in plasma, urine, and bile, *Cancer Res* 47, 2203-2206.
- [13] Reilly, R. T., Barbour, K. W., Dunlap, R. B., and Berger, F. G. (1995) Biphasic binding of 5-fluoro-2'-deoxyuridylate to human thymidylate synthase, *Mol Pharmacol* 48, 72-79.
- [14] Helsper, J. T., and Demoss, E. V. (1964) Regional Intra-Arterial Infusion of 5-Fluorouracil for Cancer, *Surgery 56*, 340-348.
- [15] Almersjo, O., Brandberg, A., and Gustavsson, B. (1975) Concentration of biologically active 5-fluorouracil in general circulation during continuous portal infusion in man: a preliminary report, *Cancer Lett 1*, 113-117.

- [16] Amstutz, U., Froehlich, T. K., and Largiader, C. R. (2011) Dihydropyrimidine dehydrogenase gene as a major predictor of severe 5-fluorouracil toxicity, *Pharmacogenomics 12*, 1321-1336.
- [17] Diasio, R. B., Beavers, T. L., and Carpenter, J. T. (1988) Familial deficiency of dihydropyrimidine dehydrogenase. Biochemical basis for familial pyrimidinemia and severe 5-fluorouracil-induced toxicity, *J Clin Invest 81*, 47-51.
- [18] Harris, B. E., Carpenter, J. T., and Diasio, R. B. (1991) Severe 5-fluorouracil toxicity secondary to dihydropyrimidine dehydrogenase deficiency. A potentially more common pharmacogenetic syndrome, *Cancer 68*, 499-501.
- [19] Rivera, E., Chang, J. C., Semiglazov, V., Burdaeva, O., Kirby, M. G., and Spector, T. (2014)

 Eniluracil plus 5-fluorouracil and leucovorin: treatment for metastatic breast cancer

 patients in whom capecitabine treatment rapidly failed, *Clin Breast Cancer 14*, 26-30.
- [20] Levin, J., and Hohneker, J. (2000) Clinical development of eniluracil/fluorouracil: an oral treatment for patients with solid tumors, *Invest New Drugs 18*, 383-390.
- [21] Diasio, R. B. (2002) Can eniluracil improve 5-fluorouracil therapy?, *Clin Colorectal Cancer 2*, 53.
- [22] Schilsky, R. L., and Kindler, H. L. (2000) Eniluracil: an irreversible inhibitor of dihydropyrimidine dehydrogenase, *Expert Opin Investig Drugs 9*, 1635-1649.
- [23] Baker, S. D. (2000) Pharmacology of fluorinated pyrimidines: eniluracil, *Invest New Drugs 18*, 373-381.

- [24] Baccanari, D. P., Davis, S. T., Knick, V. C., and Spector, T. (1993) 5-Ethynyluracil (776C85): a potent modulator of the pharmacokinetics and antitumor efficacy of 5-fluorouracil, *Proc Natl Acad Sci U S A 90*, 11064-11068.
- [25] Spector, T., Harrington, J. A., and Porter, D. J. (1993) 5-Ethynyluracil (776C85): inactivation of dihydropyrimidine dehydrogenase in vivo, *Biochem Pharmacol* 46, 2243-2248.
- [26] Rowinsky, E. K. (1995) The suitability of selected new anticancer agents for infusional therapy and the effects of others on infusional therapy practices, *J Infus Chemother 5*, 173-178.
- [27] Milano, G., Etienne, M. C., and Fischel, J. L. (1995) [Intratumoral dihydropyrimidine dehydrogenase and its inhibition: a new approach in the pharmacokinetics of 5-fluorouracil], *Ann Gastroenterol Hepatol (Paris)* 31, 103-105.
- [28] Cao, S., Baccanari, D. P., Joyner, S. S., Davis, S. T., Rustum, Y. M., and Spector, T. (1995) 5-Ethynyluracil (776C85): effects on the antitumor activity and pharmacokinetics of tegafur, a prodrug of 5-fluorouracil, *Cancer Res 55*, 6227-6230.
- [29] Baker, S. D., Diasio, R. B., O'Reilly, S., Lucas, V. S., Khor, S. P., Sartorius, S. E., Donehower, R. C., Grochow, L. B., Spector, T., Hohneker, J. A., and Rowinsky, E. K. (2000) Phase I and pharmacologic study of oral fluorouracil on a chronic daily schedule in combination with the dihydropyrimidine dehydrogenase inactivator eniluracil, *J Clin Oncol* 18, 915-926.
- [30] Grem, J. L., Harold, N., Shapiro, J., Bi, D. Q., Quinn, M. G., Zentko, S., Keith, B., Hamilton, J. M., Monahan, B. P., Donavan, S., Grollman, F., Morrison, G., and Takimoto, C. H. (2000)
 Phase I and pharmacokinetic trial of weekly oral fluorouracil given with eniluracil and low-dose leucovorin to patients with solid tumors, *J Clin Oncol 18*, 3952-3963.

- [31] Schilsky, R. L., Bukowski, R., Burris, H., 3rd, Hochster, H., O'Rourke, M., Wall, J. G., Mani, S., Bonny, T., Levin, J., and Hohneker, J. (2000) A multicenter phase II study of a five-day regimen of oral 5-fluorouracil plus eniluracil with or without leucovorin in patients with metastatic colorectal cancer, *Ann Oncol* 11, 415-420.
- [32] Skovsgaard, T., Davidson, N. G., Piccart, M. J., Richel, D. J., Bonneterre, J., Cirkel, D. T., Barton, C. M., and Eniluracil/Fluorouracil Breast Cancer Study, G. (2001) A phase II study of oral eniluracil/fluorouracil in patients with anthracycline-refractory or anthracycline- and taxane-refractory advanced breast cancer, *Ann Oncol* 12, 1255-1257.
- [33] Leichman, C. G., Chansky, K., Macdonald, J. S., Doukas, M. A., Budd, G. T., Giguere, J. K., Abbruzzese, J. L., and Southwest Oncology, G. (2002) Biochemical modulation of 5-fluorouacil through dihydropyrimidine dehydrogenase inhibition: a Southwest Oncology Group phase II trial of eniluracil and 5-fluorouracil in advanced resistant colorectal cancer, *Invest New Drugs 20*, 419-424.
- [34] Heslin, M. J., Yan, J., Weiss, H., Shao, L., Owens, J., Lucas, V. S., and Diasio, R. B. (2003)

 Dihydropyrimidine dehydrogenase (DPD) rapidly regenerates after inactivation by eniluracil (GW776C85) in primary and metastatic colorectal cancer, *Cancer Chemother Pharmacol* 52, 399-404.
- [35] de Bono, J. S., and Twelves, C. J. (2001) The oral fluorinated pyrimidines, *Invest New Drugs* 19, 41-59.
- [36] Diasio, R. B. (2002) An evolving role for oral fluoropyrimidine drugs, J Clin Oncol 20, 894-896.
- [37] Saltz, L., Shimada, Y., and Khayat, D. (1996) CPT-11 (irinotecan) and 5-fluorouracil: a promising combination for therapy of colorectal cancer, *Eur J Cancer 32A Suppl 3*, S24-31.

- [38] Kobayashi, K., Shinbara, A., Kamimura, M., Takeda, Y., Kudo, K., Kabe, J., Hibino, S., Hino, M., Shibuya, M., and Kudoh, S. (1998) Irinotecan (CPT-11) in combination with weekly administration of cisplatin (CDDP) for non-small-cell lung cancer, *Cancer Chemother Pharmacol* 42, 53-58.
- [39] Rothenberg, M. L., Cox, J. V., DeVore, R. F., Hainsworth, J. D., Pazdur, R., Rivkin, S. E., Macdonald, J. S., Geyer, C. E., Jr., Sandbach, J., Wolf, D. L., Mohrland, J. S., Elfring, G. L., Miller, L. L., and Von Hoff, D. D. (1999) A multicenter, phase II trial of weekly irinotecan (CPT-11) in patients with previously treated colorectal carcinoma, *Cancer 85*, 786-795.
- [40] Fujishiro, M., Shinkai, T., Fukuda, M., Tamura, T., Ohe, Y., Kunitoh, H., Nishiwaki, Y., Sekine, I., Fukuda, H., and Saijo, N. (2000) Phase I study of a weekly infusion of irinotecan hydrochloride (CPT-11) and a 14-day continuous infusion of etoposide in patients with lung cancer: JCOG trial 9408, *Jpn J Clin Oncol 30*, 487-493.
- [41] Spector, T., and Cao, S. (2010) A possible cause and remedy for the clinical failure of 5-fluorouracil plus eniluracil, *Clin Colorectal Cancer 9*, 52-54.
- [42] Barr, P. J., Jones, A. S., and Walker, R. T. (1976) Incorporation of 5-substituted uracil derivatives into nucleic acids. Part IV. The synthesis of 5-ethynyluracil, *Nucleic Acids Res* 3, 2845-2849.
- [43] Schroeder, A. C., Bloch, A., Perman, J. L., and Bobek, M. (1982) Synthesis and biological evaluation of 6-ethynyluracil, a thiol-specific alkylating pyrimidine, *J Med Chem 25*, 1255-1258.

- [44] Porter, D. J., Chestnut, W. G., Merrill, B. M., and Spector, T. (1992) Mechanism-based inactivation of dihydropyrimidine dehydrogenase by 5-ethynyluracil, *J Biol Chem 267*, 5236-5242.
- [45] Beaupre, B. A., Hoag, M. R., Roman, J., Forsterling, F. H., and Moran, G. R. (2015) Metabolic Function for Human Renalase: Oxidation of Isomeric Forms of beta-NAD(P)H that Are Inhibitory to Primary Metabolism, *Biochemistry 54*, 795-806.
- [46] Beaupre, B. A., Roman, J. V., and Moran, G. R. (2020) An improved method for the expression and purification of porcine dihydropyrimidine dehydrogenase, *Protein Expr Purif* 171, 105610.
- [47] Rosenbaum, K., Schaffrath, B., Hagen, W. R., Jahnke, K., Gonzalez, F. J., Cook, P. F., and Schnackerz, K. D. (1997) Purification, characterization, and kinetics of porcine recombinant dihydropyrimidine dehydrogenase, *Protein Expr Purif* 10, 185-191.
- [48] Rosenbaum, K., Jahnke, K., Curti, B., Hagen, W. R., Schnackerz, K. D., and Vanoni, M. A. (1998)

 Porcine recombinant dihydropyrimidine dehydrogenase: comparison of the spectroscopic and catalytic properties of the wild-type and C671A mutant enzymes, *Biochemistry 37*, 17598-17609.
- [49] Beaupre, B. A., Forouzesh, D. C., and Moran, G. R. (2020) Transient-State Analysis of Porcine

 Dihydropyrimidine Dehydrogenase Reveals Reductive Activation by NADPH, *Biochemistry*59, 2419-2431.
- [50] Moran, G. R. (2019) Anaerobic methods for the transient-state study of flavoproteins: The use of specialized glassware to define the concentration of dioxygen, *Methods Enzymol* 620, 27-49.

- [51] Holzer, W., Shirdel, J., Zirak, P., Penzkofer, A., Hegemann, P., Deutzmann, R., and Hochmuth,
 E. (2005) Photo-induced degradation of some flavins in aqueous solution, *Chemical Physics* 308, 69-78.
- [52] Winter, G. (2010) xia2: an expert system for macromolecular crystallography data reduction, *J Appl Crystallogr 43*, 186-190.
- [53] Winn, M. D., Ballard, C. C., Cowtan, K. D., Dodson, E. J., Emsley, P., Evans, P. R., Keegan, R. M., Krissinel, E. B., Leslie, A. G., McCoy, A., McNicholas, S. J., Murshudov, G. N., Pannu, N. S., Potterton, E. A., Powell, H. R., Read, R. J., Vagin, A., and Wilson, K. S. (2011) Overview of the CCP4 suite and current developments, *Acta Crystallogr D Biol Crystallogr 67*, 235-242.
- [54] Liebschner, D., Afonine, P. V., Baker, M. L., Bunkoczi, G., Chen, V. B., Croll, T. I., Hintze, B., Hung, L. W., Jain, S., McCoy, A. J., Moriarty, N. W., Oeffner, R. D., Poon, B. K., Prisant, M. G., Read, R. J., Richardson, J. S., Richardson, D. C., Sammito, M. D., Sobolev, O. V., Stockwell, D. H., Terwilliger, T. C., Urzhumtsev, A. G., Videau, L. L., Williams, C. J., and Adams, P. D. (2019) Macromolecular structure determination using X-rays, neutrons and electrons: recent developments in Phenix, Acta Crystallogr D Struct Biol 75, 861-877.
- [55] McCoy, A. J., Grosse-Kunstleve, R. W., Adams, P. D., Winn, M. D., Storoni, L. C., and Read, R. J. (2007) Phaser crystallographic software, *J Appl Crystallogr* 40, 658-674.
- [56] Emsley, P., Lohkamp, B., Scott, W. G., and Cowtan, K. (2010) Features and development of Coot, *Acta Crystallogr D Biol Crystallogr 66*, 486-501.
- [57] Lowe, A. B. (2014) Thiol-yne 'click'/coupling chemistry and recent applications in polymer and materials synthesis and modification, *Polymer 55*, 5517-5549.

- [58] Hoag, M. R., Roman, J., Beaupre, B. A., Silvaggi, N. R., and Moran, G. R. (2015) Bacterial Renalase: Structure and Kinetics of an Enzyme with 2- and 6-Dihydro-beta-NAD(P)

 Oxidase Activity from Pseudomonas phaseolicola, *Biochemistry* 54, 3791-3802.
- [59] Lowry, O. H., Passonneau, J. V., and Rock, M. K. (1961) The stability of pyridine nucleotides, *The Journal of biological chemistry 236*, 2756-2759.
- [60] Porter, D. J., Chestnut, W. G., Taylor, L. C., Merrill, B. M., and Spector, T. (1991) Inactivation of dihydropyrimidine dehydrogenase by 5-iodouracil, *J Biol Chem 266*, 19988-19994.
- [61] Rohr, A. K., Hersleth, H. P., and Andersson, K. K. (2010) Tracking flavin conformations in protein crystal structures with Raman spectroscopy and QM/MM calculations, *Angew Chem Int Ed Engl 49*, 2324-2327.

Acknowledgements

This research was supported by Loyola University College of Arts and Sciences and National Science Foundation Grant 1904480 to G.R.M.

Uniprot Identifiers

Sus Scrofa DPD - Q28943

For Table of Contents use only

